Applied Physics Letters

Plasmon gap mode-assisted third-harmonic generation from metal film-coupled nanowires

Cite as: Appl. Phys. Lett. **104**, 261105 (2014); https://doi.org/10.1063/1.4886409
Submitted: 30 April 2014 . Accepted: 20 June 2014 . Published Online: 01 July 2014

Ke Li, Xiaofeng Li, Dang Yuan Lei, Shaolong Wu, and Yaohui Zhan

Plasmon gap mode-assisted third-harmonic generation from metal film-coupled nanowires

Ke Li,[1,2] Xiaofeng Li,[1,2,a)] Dang Yuan Lei,[3,4] Shaolong Wu,[1,2] and Yaohui Zhan[1,2]
[1]*College of Physics, Optoelectronics and Energy & Collaborative Innovation Center of Suzhou Nano Science and Technology, Soochow University, Suzhou 215006, China*
[2]*Key Lab of Advanced Optical Manufacturing Technologies of Jiangsu Province & Key Lab of Modern Optical Technologies of Education Ministry of China, Soochow University, Suzhou 215006, China*
[3]*Department of Applied Physics, The Hong Kong Polytechnic University, Hong Kong, China*
[4]*Shenzhen Research Institute, The Hong Kong Polytechnic University, Shenzhen 518057, China*

(Received 30 April 2014; accepted 20 June 2014; published online 1 July 2014)

A numerical investigation on the third-order nonlinear optical properties of a plasmonic system composed by metal film-coupled nanowires is reported. The linear and nonlinear optical characteristics are studied by finite-difference time-domain (FDTD) method. To substantially improve the nonlinear effect, the geometric parameters of the system are carefully engineered to excite strong plasmon gap resonance with dramatically enhanced electric field intensity at the gap between the nanowires and the film. The third-harmonic generation (THG) property is examined by nonlinear FDTD simulation. It shows that the THG efficiency estimated from the nonlinear optical absorption can be $\sim 1 \times 10^{-5}$ under an incident power density of 5.2 GW/cm^2. Plasmonic resonance is necessary to achieve highly efficient THG since the system on resonance shows the THG intensity 4 orders of magnitude higher than that of an off-resonance system. © *2014 AIP Publishing LLC*. [http://dx.doi.org/10.1063/1.4886409]

With the rapid development of nanofabrication technique, nonlinear effects of metallic micro/nanostructures have attracted much attention, which significantly enrich the applications of nanophotonic devices beyond the linear systems.[1,2] Metallic nanostructures support collective oscillations of conduction electrons, i.e., surface plasmon polaritons (SPPs), which dramatically squeeze and localize the optical energy within an ultra-small mode volume. The efficient nanoscale light concentration facilitates the light harness and enhances the nonlinear optical processes in metallic nanostructures, including photovoltaic devices[3–5] and second/third harmonic generation (SHG/THG).[6,7]

To get stronger optical harmonic generation, effective nanodesign is usually a decisive factor since the nonlinear susceptibility is inherently weak.[8] SPPs provide therefore a perfect means to fulfill the stringent requirement of strong field localization and energy density concentration for efficient nonlinear optical process. Early studies of surface enhanced SHG considered a smooth/rough metal surface/grating.[9,10] Metallic nanostructures, including bowties, nanocups, and split-ring resonators (SRRs), were fabricated to amplify various nonlinear optical effects. It was reported that SHG efficiency from a doubly resonant metallic bowtie hole array can reach 1.4×10^{-8},[11] while that from a nanocup structure can be 1.8×10^{-9}.[12] The SRR system obtains even higher efficiency, i.e., 2×10^{-6} (2×10^{-7}) for THG (SHG).[13] More recently, the third-harmonic-upconversion from an indium tin oxide nanoparticle decorated with a plasmonic dimer was fabricated by electron-beam lithography, leading to efficiency up to 0.0007%.[14]

In this work, we propose a simple plasmonic gap system composed by metal film-coupled nanowires (NWs),[15] where nonlinearities of both metal and gap material are employed to enhance the THG efficiency effectively. Both linear and nonlinear optical responses of the system are investigated based on the finite-difference time-domain (FDTD) method (Lumerical, Inc.). Benefiting from the examination of the linear response, the plasmonic resonance is carefully tuned by engineering the NW radius and spacer thickness, resulting in a local field intensity enhancement over 2500 times at the target frequency (ω). The nonlinear response with system parameters optimized from linear optical design is then studied by a user-modified nonlinear electromagnetic simulation code. It shows that the frequency-tripling efficiencies (from ω to 3ω) evaluated from the system absorption and reflection can be close to 1×10^{-5} and 1×10^{-6}, respectively. Finally, a detailed comparison between THG responses with on- and off-resonance configurations is given, confirming the key role of plasmonic resonance in enhancing the THG efficiency.

A specific example of metal-film-coupled NWs is illustrated in Fig. 1. The NWs (radius: R) and metallic film are made of gold,[16] while the spacer is poly-methyl methacrylate (PMMA, thickness: d) with the substrate of SiO_2. The material index is fitted in the simulation in a polynomial way with material dispersion included. The period of NW array and the thickness of gold film are 800 and 100 nm, respectively. Only transverse magnetic (TM) incidence is considered in order to excite the plasmon gap modes (transverse electric incidence does not yield strong THG with the absence of SPPs). Symmetric boundary condition is used, which can accurately simulate the interested periodic system with a much fast computational speed. As the localized SPPs occur near the gap between the NWs and the metal film, the nearby

[a)]Author to whom correspondence should be addressed. Electronic mail: xfli@suda.edu.cn

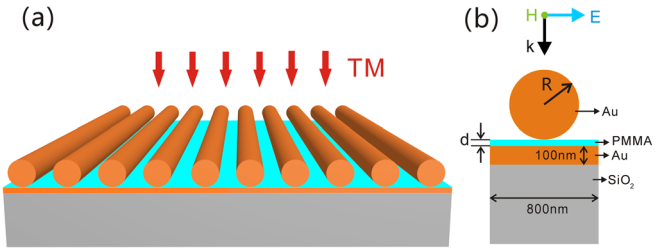

FIG. 1. Schematic sketch of gold film-coupled nanowires (radius: *R)* with an intermediate spacer of PMMA (thickness: *d*). The TM-polarized light illuminates the structure at normal incidence. (a) Three-dimensional view of the whole structure and (b) cross-sectional view of one period.

mesh is set as fine as 1 nm in the simulation to render the field distribution precisely. The narrow band light injection is around the wavelength of 1.2 μm (ω), which yields the third-harmonic component at round 400 nm (3ω).

In order to substantially enhance the THG process, the electric field at ω must be as strong as possible, which can be realized by plasmonic designs. Therefore, the linear response has to be first examined to quantify the local field intensity at $\lambda = 1.2\,\mu$m. In the interested plasmonic system, the strongly enhanced localized field is arisen from the plasmonic resonance, which is in turn accompanied by the absorption peaks under the extremely strong and in-phase light-device coupling; therefore, we focus on the means of spectrally positioning and maximizing the absorption through linear optical design. By calculating the reflection (Ref) and transmission (Tra) of the system through integrating the power density over the interface in the front and rear sides and being normalized with respect to the source power, P_{abs} can be calculated: $P_{abs} = 1 - \text{Ref} - \text{Tra}$. Since the bottom gold film is sufficiently thick, $P_{abs} \sim 1 - \text{Ref}$.

Plotted in Fig. 2(a) shows how the P_{abs} can be tuned by controlling R, where R is from 50 to 395 nm with equally spaced 50 values, λ is from 0.2 to 2 μm with equally spaced 400 values, and $d = 5$ nm. One can see that at $P_{abs} > 80\%$ when $\lambda \leq 0.5\,\mu$m, almost independent of R due to the interband absorption of gold. In longer wavelength regime ($0.8 \leq \lambda \leq 1.5\,\mu$m), an absorption peak appears and red-shifts with increasing R. For $R \geq 200$ nm, higher-order resonant modes are excited and coexist with the low-order mode. It is thus extremely important to determine R for the target wavelength as the degree of field enhancement is strongly attributed to the system absorption. For example, for a plasmonic resonance at $\lambda = 1.2\,\mu$m, $R = 250$ nm has to be used. In Fig. 2(b), the dependence of P_{abs} spectrum on the spacer thickness is examined, where $R = 250$ nm and d is from 4 to 100 nm with the step of 2 nm. It is obvious that the two low-order plasmonic modes are excited simultaneously and show slight blue-shifts with increasing d from 4 to 10 nm; however, further increasing d does not noticeably shift the resonances any more but greatly weakens the light absorptivity. This is because: with the NWs moving away from the Au film, (1) the effective index governing the plasmonic resonance is decreased, leading to the blue-shifted resonance; (2) the NW-film coupling is lower and the gap modes become much weaker with a significantly reduced P_{abs}; (3) when d is large enough, the presence of Au film does not qualitatively modify the environmental refractive index surrounding the NWs, resulting in the stabilized resonant wavelength. The dependences of P_{abs} at $\lambda = 1.2\,\mu$m upon R and d are displayed in

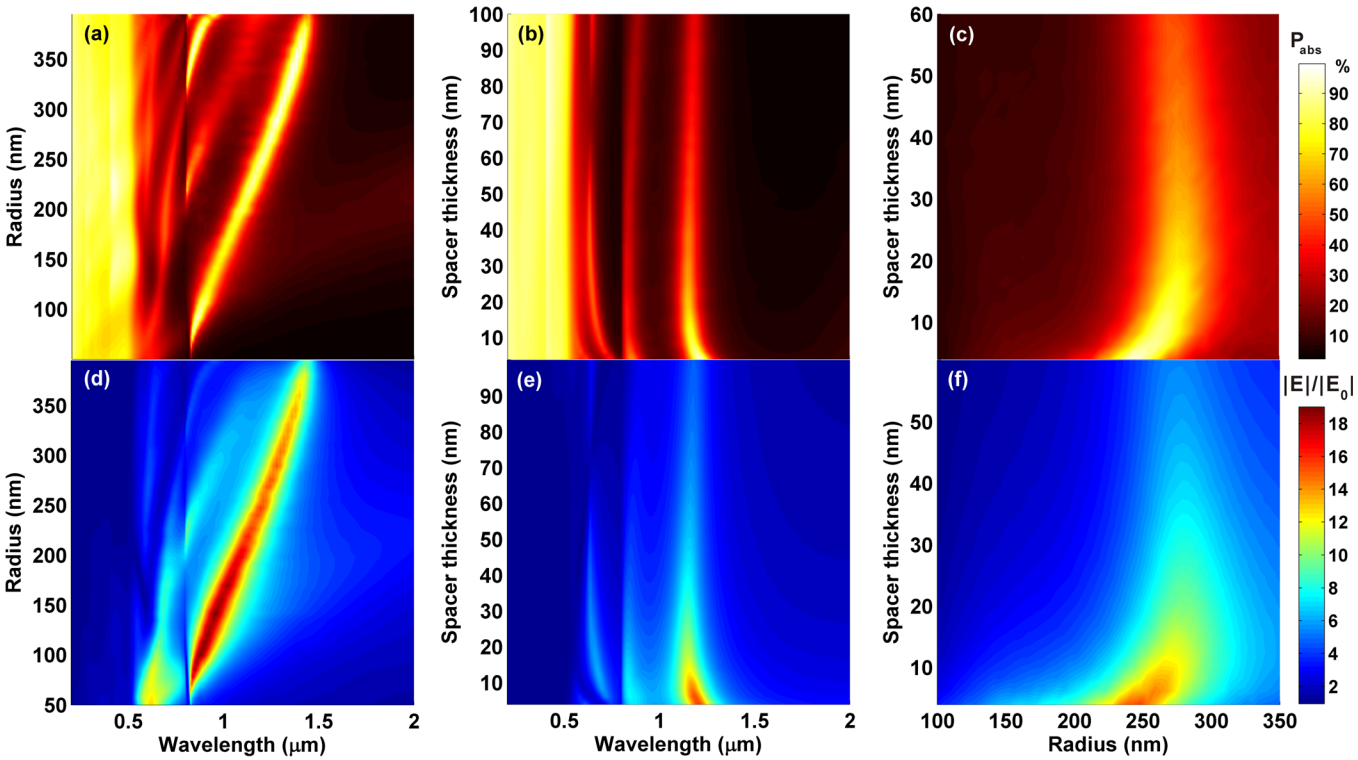

FIG. 2. (a) and (d) Contour plot of P_{abs} [$|E|/|E_0|$] versus NW radius and incident wavelength at $d = 5$ nm. (b) and (e) Contour plot of P_{abs} [$|E|/|E_0|$] as versus spacer thickness and incident wavelength at $R = 250$ nm. (c) and (f) Contour plot of P_{abs} [$|E|/|E_0|$] versus nanowire radius and spacer thickness at $\lambda = 1.2\,\mu$m. The electric field is taken from a specified point shifted horizontally by $R/4$ from the gap center.

Fig. 2(c), showing that a narrow gap is desired for the strongest absorption.

The controllability of field enhancement $|E|/|E_0|$ by R and d is further studied, where E (E_0) are the spatially localized (source) electric fields [Figs. 2(d)–2(f)]. The calculated E is not the highest value in the system, but from a specified point (by a point monitor) shifted horizontally by $R/4$ from the gap center. This is to avoid using a high-dimensional monitor with a huge amount of data, especially under such a large number of parametrical sweeps. This treatment is rational since the fields elsewhere show similar response with varying R and d. According to Fig. 2, the electric field behaves with a very similar manner as P_{abs}, showing that the linear optical design based on P_{abs} is effective in finding the best candidates for a strong nonlinear response.

According to Figs. 2(a)–2(c), a very strong P_{abs} at $\lambda = 1.2\ \mu m$ can be obtained by setting $R = 250\,nm$ and $d = 5\,nm$. The absorptivity spectrum is shown in Fig. 3(a), where $P_{abs} \sim 92\%$ at $\lambda = 1.2\ \mu m$ with another peak $\sim 54\%$ at $0.85\ \mu m$. The corresponding spatial patterns of $|E|/|E_0|$ are shown in Figs. 3(b) and 3(c), respectively. It is seen that the maximal amplitude enhancement of the electric field at $0.85\ \mu m$ is about 30 times, while it is over 50 times at $1.2\ \mu m$, i.e., leading to an intensity enhancement factor ($\propto |E|^2$) over 2500 for Fig. 3(c) and 900 for Fig. 3(b). These patterns verify that the resonance occurring at $0.85\ \mu m$ is originated from the higher-order plasmonic mode with a lower energy concentration, contributing lower nonlinear conversion efficiency. Plotted in Fig. 3(d) is the field pattern of the system under off-resonance condition, e.g., $\lambda = 1.5\ \mu m$. It is obvious that the non-plasmonic field is much weaker, which cannot guarantee a strong nonlinear process as discussed later.

Realizing plasmon gap-mode-induced field enhancement, we now turn our attention to the nonlinear optical response from the system. The electric polarization can be written as

$$\vec{P}(\vec{r},t) = \varepsilon_0\chi^{(1)} \cdot \vec{E} + \varepsilon_0\chi^{(2)} : \vec{E}\vec{E} + \varepsilon_0\chi^{(3)} \vdots \vec{E}\vec{E}\vec{E} + \ldots \quad (1)$$

The first term on the right side is the linear polarization, while the rest represent the basic sources of nonlinear optical effects under different orders. The values for $\chi^{(n)}$ with $n > 3$ are negligible due to the weak high-order nonlinearity. Moreover, we choose not to contain the geometry-induced weak second order contribution,[17–19] since it does not noticeably affect the THG besides introducing more frequency components. To fully using the strongly enhanced field around the gap, nonlinearities of both Au and PMMA are considered by $\chi^{(3)} = 7.56 \times 10^{-19}$ (4×10^{-22}) m^2/V^2 for Au[18] (PMMA).[20]

In our nonlinear simulations, a TM incidence with an extremely narrow line-width ($\sim 5.3\,nm$) peaked at $\lambda = 1.2\ \mu m$ is used. This is necessary since the generated harmonics are very weak compared to the source which therefore has to be very spectrally clean. A broadband monitor covering $0.2–1.8\ \mu m$ is used to detect the frequency components from nonlinear processes. Moreover, the source intensity should be well controlled with considering the damage threshold (DT) of the system. As Au has a much higher DT than PMMA,[21] the latter determines the upper limit of the incident power density. However, quite different values of DT for PMMA have been reported. For example, the single-shot DT of PMMA at $1.06\ \mu m$ is reported to be $13\,GW/cm^2$ from a 125 ps-wide pulse;[22] DT up to $1550\,GW/cm^2$ has been shown in Ref. 23. Moreover, as we know DT is raised under the illumination of a shorter laser pulse or a longer wavelength, showing that the value of DT for the considered system should be even higher. In addition, for the plasmonic system, the localized field enhancement has also to be taken into account since it yields strong local power density and reduces the upper limit of the source intensity. With considering all these mechanisms as well as the experimental evidence from Ref. 13, $5.2\,GW/cm^2$ is thus believed to be a safe power density without damaging the sample, although the incidence can actually be stronger.

The nonlinear performance is evaluated through examining both the system reflection/transmission [21–23] and the device absorption. Actually in a nonlinear system the light

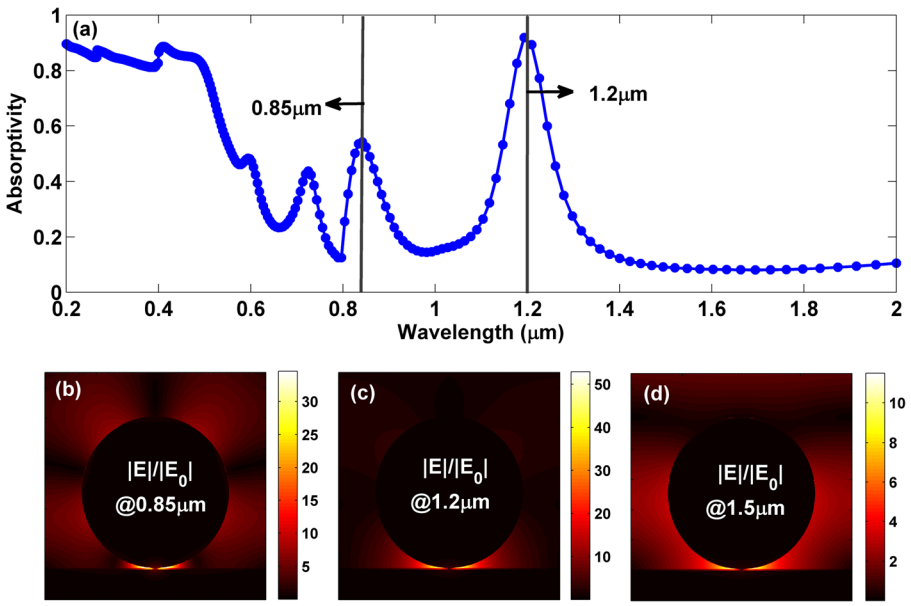

FIG. 3. (a) Absorption spectrum for the structure with $R = 250\,nm$ and $d = 5\,nm$. Cross-sectional views of electric field enhancement at $\lambda = 0.85\ \mu m$ [(b), on-resonance], $1.2\ \mu m$ [(c), on-resonance], and $1.5\ \mu m$ [(d), off-resonance].

absorptance is not straightforwardly accessible based on $P_{\text{abs}} = 1 - \text{Ref} - \text{Tra}$ as in the linear treatment since the source has a narrow band without containing the harmonic components for a good signal-to-noise ratio. The power absorbed has to be obtained by[24]

$$P_{abs} = \frac{1}{2}\oiint_V \omega\varepsilon''|E|^2 dv, \tag{2}$$

where ε'' is the imaginary part of the material permittivity and V is the device volume. Actually, evaluating the nonlinearity in terms of the device absorption can better score the nonlinear generation capability since there is a big discrepancy between the detected harmonic light in reflection and that actually generated from the plasmonic system.

In Fig. 4(a), the red/black curves illustrate the absorption/reflection spectra of THG. The peak at wavelength of 1.2 (0.4) μm is the fundamental (third-harmonic) component, while that at 0.24 μm belongs to the 5th-order harmonic component attributed to four-wave mixing, i.e., $\omega+\omega+3\omega=5\omega$. The inset in Fig. 4(a) shows the spectral details around the THG peak. It is observed that the peak reflection power of THG at 3ω is over one order of magnitude smaller than that of the absorption, due to the near-field nature of the localized SPPs and the strong metallic parasitic absorption.

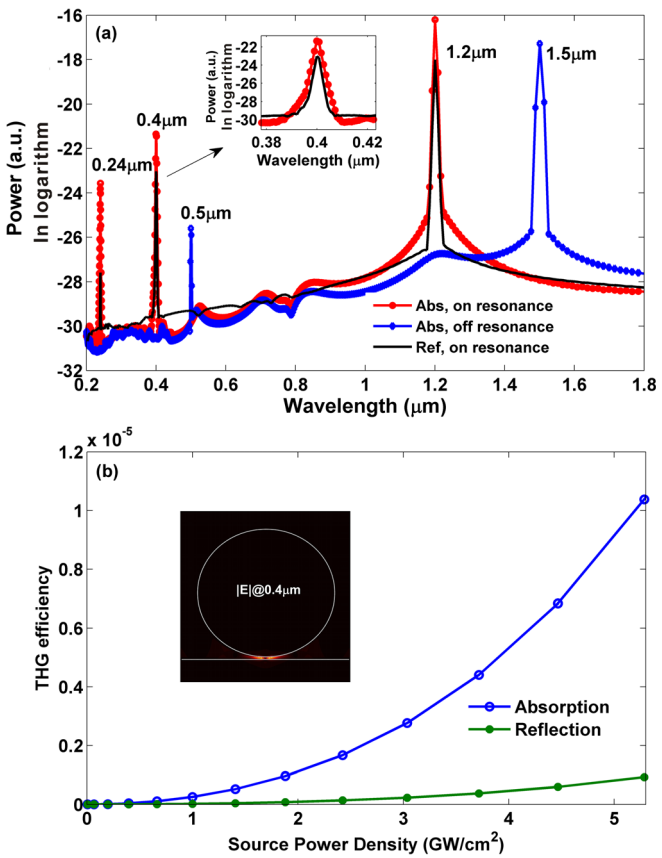

FIG. 4. (a) Absorption and reflection spectral response of the THG from the gold film-coupled nanowires at $d = 5$ nm and $R = 250$ nm. The inset is the spectral details around the THG peak. (b) THG efficiency of absorption and reflection as a function of source power density. The inset is the electric field distribution at third harmonic emission wavelength (0.4 μm).

This brings an open and crucial question for plasmonic nonlinear systems, i.e., how to couple efficiently the generated strong harmonic light out of the device and suppress the metallic absorption loss,[25,26] i.e., the key reason for the experimentally observed low nonlinear generation efficiency.[11,12] The source power density could be calculated as P_{ω}. Hence, the ratio of $P_{3\omega}$ and P_{ω} produces the frequency conversion efficiency of THG. Fig. 4(b) illustrates the THG efficiency of absorption and reflection as a function of source power density. The THG efficiency of reflection can reach 1×10^{-6}, while that of absorption can be close to 1×10^{-5} when the incident power density is 5.2 GW/cm^2. Inset in Fig. 4(b) is the spatial pattern of the third harmonic electric field from nonlinear optical simulation, which inherits the character of the ω-component (Fig. 3) and confirms the importance of resonance condition at ω. These results indicate that the metal film-coupled NW system can indeed significantly enhance the THG through the strong field localization enabled by plasmon gap mode.

We finally compare the THG performance of the system under on- and off-resonance. According to Fig. 3, the plasmon gap mode resonance can be achieved at $\lambda = 1.2$ μm (on-resonance); nevertheless, much lower P_{abs} is observed at $\lambda = 1.5$ μm (off-resonance). In this simulation, two narrowband light sources with peak wavelengths at 1.2 and 1.5 μm with an identical source intensity are introduced. The monitor spectral band is from 0.2 to 1.8 μm with the system configuration unchanged. Fig. 4(a) shows that, besides the components at 1.2 and 1.5 μm, the corresponding third-harmonic ones are observed at 0.4 and 0.5 μm, respectively; moreover, the 3ω intensity at 0.5 μm (off-resonance) is about 4 orders of magnitude lower than that at 0.4 μm (on-resonance). In fact, the direct comparison between the 3ω intensity (Fig. 4) and the electric field enhancement (Fig. 3) clearly reveals that the plasmon resonance plays a crucial role in enhancing the nonlinear frequency conversion capability. In other words, with the nonlinear material predetermined, the efficiency of nonlinear optical processes in plasmonic nanostructures is mainly determined by how strong the localized field can be achieved. This also points out that the plasmonic structures such as metal nanocrescents[27] and kissing cylinders,[28,29] which have demonstrated huge field enhancement, could give rise to even higher THG efficiency.

In conclusion, the metal film-coupled nanowire system has been studied using FDTD method, via which both linear and nonlinear optical responses are calculated. Through carefully tuning the plasmon gap mode resonance and engineering the NW-film gap, strong localized electric field is achieved, which greatly enhances the nonlinear optical process. Our nonlinear electromagnetic simulation shows that the THG efficiency can be close to 1×10^{-6} and 1×10^{-5} evaluated from the reflection and absorption spectra, respectively. The comparison of the nonlinear response of the systems under on- and off-resonance configurations reveals that plasmonic resonance is extremely effective in enhancing the THG efficiency. Moreover, we have addressed an important issue, i.e., the obvious discrepancy between the detectable reflection and the device parasitic absorption, which constraints the nonlinear conversion efficiency. This opens a question for the design

of systems with much improved out-coupling efficiency for higher system performance.[25,26]

This work was supported by NSFC (Nos. 91233119 and 61204066), Ph.D. Programs Foundation of Ministry of Education of China (No. 20133201110021), and Priority Academic Program Development (PAPD) of Jiangsu Higher Education Institutions. D. Y. Lei acknowledges the support by the Hong Kong Research Grants Council (ECS Grant No. 509513) and NSFC (No. 11304261).

[1]R. F. Oulton, V. J. Sorger, D. A. Genov, D. F. P. Pile, and X. Zhang, Nat. Photonics **2**, 496 (2008).
[2]M. L. Brongersma, Nat. Photonics **2**, 270 (2008).
[3]X. Li, N. Hylton, V. Giannini, K.-H. Lee, N. J. Ekins-Daukes, and S. A. Maier, Opt. Express **19**, 888 (2011).
[4]X. Li, N. Hylton, V. Giannini, K.-H. Lee, N. J. Ekins-Daukes, and S. A. Maier, Prog. Photovoltaics: Res. Appl. **21**, 109 (2013).
[5]N. P. Hylton, X. Li, V. Giannini, K. H. Lee, N. J. Ekins-Daukes, J. Loo, D. Vercruysse, P. Van Dorpe, H. Sodabanlu, M. Sugiyama, and S. A. Maier, Sci. Rep. **3**, 2874 (2013).
[6]H. Aouani, M. Navarro-Cia, M. Rahmani, T. P. H. Sidiropoulos, M. Hong, R. F. Oulton, and S. A. Maier, Nano Lett. **12**, 4997 (2012).
[7]S. Chen, W. Wong, Y. Pun, K. Cheah, and G. Li, Adv. Opt. Mater. **1**, 522 (2013).
[8]J. E. Sipe, V. C. Y. So, M. Fukui, and G. I. Stegeman, Phys. Rev. B **21**, 4389 (1980).
[9]C. K. Chen, A. R. B. Decastro, and Y. R. Shen, Phys. Rev. Lett. **46**, 145 (1981).
[10]A. Nahata, R. A. Linke, T. Ishi, and K. Ohashi, Opt. Lett. **28**, 423 (2003).
[11]S. Park, J. W. Hahn, and J. Y. Lee, Opt. Express **20**, 4856 (2012).
[12]C. M. Soukoulis and M. Wegener, Nat. Photonics **5**, 523 (2011).
[13]M. W. Klein, M. Wegener, N. Feth, and S. Linden, Opt. Express **15**, 5238 (2007).
[14]H. Aouani, M. Rahmani, M. Navarro-Cia, and S. A. Maier, Nat. Nanotechnol. **9**, 290 (2014).
[15]D. Y. Lei, A. I. Fernandez-Dominguez, Y. Sonnefraud, K. Appavoo, R. F. Haglund, J. B. Pendry, and S. A. Maier, ACS Nano **6**, 1380 (2012).
[16]P. B. Johnson and R. W. Christy, Phys. Rev. B **6**, 4370 (1972).
[17]C. Ciraci, E. Poutrina, M. Scalora, and D. R. Smith, Phys. Rev. B **86**, 115451 (2012).
[18]F. X. Wang, F. J. Rodriguez, W. M. Albers, R. Ahorinta, J. E. Sipe, and M. Kauranen, Phys. Rev. B **80**, 233402 (2009).
[19]Y. Zeng, W. Hoyer, J. J. Liu, S. W. Koch, and J. V. Moloney, Phys. Rev. B **79**, 235109 (2009).
[20]F. D'Amore, M. Lanata, S. M. Pietralunga, M. C. Gallazzi, and G. Zerbi, Opt. Mater. **24**, 661 (2004).
[21]A. M. Summer, A. S. Ramm, G. Paneru, M. F. Kling, B. N. Flanders, and C. A. Trallero-Herrero, Opt. Express **22**, 4235 (2014).
[22]R. M. O'Connell, T. F. Deaton, and T. T. Saito, Appl. Opt. **23**, 682 (1984).
[23]M. P. Felix and W. Nachbar, Appl. Phys. Lett. **25**, 25 (1974).
[24]X. Li and Y. Zhan, Appl. Phys. Lett. **102**, 021101 (2013).
[25]M. Navarro-Cia and S. A. Maier, ACS Nano **6**, 3537 (2012).
[26]U. K. Chettiar and N. Engheta, Phys. Rev. B **86**, 075405 (2012).
[27]A. Aubry, D. Y. Lei, A. I. Fernández-Domínguez, Y. Sonnefraud, S. A. Maier, and J. B. Pendry, Nano Lett. **10**, 2574 (2010).
[28]D. Y. Lei, A. Aubry, S. A. Maier, and J. B. Pendry, New J. Phys. **12**, 093030 (2010).
[29]D. Y. Lei, A. Aubry, Y. Luo, S. A. Maier, and J. B. Pendry, ACS Nano **5**, 597 (2011).